

Mechanical spectroscopy study in commercial grain oriented silicon steel

O. A. LAMBRI

Member of the CONICET's research staff, Instituto de Física Rosario, Avda. 27 de febrero 210 bis, (2000) Rosario, Argentina; Escuela de Ingeniería Eléctrica, Facultad de Ciencias Exactas, Ingeniería y Agrimensura, Universidad Nacional de Rosario, Avda Pellegrini 250 (2000) Rosario, Argentina
E-mail: olambri@fceia.unr.edu.ar

E. D. BULEJES

Escuela de Ingeniería Eléctrica, Facultad de Ciencias Exactas, Ingeniería y Agrimensura, Universidad Nacional de Rosario, Avda Pellegrini 250 (2000) Rosario, Argentina

P. GORRIA

Departamento de Física, Universidad de Oviedo, Avda. Calvo Sotelo, s/n, E-33007 Oviedo, Spain

R. J. TINIVELLA

Escuela de Ingeniería Eléctrica, Facultad de Ciencias Exactas, Ingeniería y Agrimensura, Universidad Nacional de Rosario, Avda Pellegrini 250 (2000) Rosario, Argentina; Universidad Tecnológica Nacional, Secretaría de Ciencia y Técnica, Facultad Regional Rosario, Zeballos 1341, (2000) Rosario, Argentina

Mechanical spectroscopy measurements were performed in commercial grain oriented silicon steel to study the outstanding features of modulus and damping spectrum. A relation between the features of the damping and modulus behaviour with the grain boundaries characteristics will be established. It should be pointed out that the elastic modulus shows an anomalous step at around 800 K. The physical mechanism involved in this process will be studied. A cooperative mechanism involving dislocations will be proposed. Besides this, the magnetic characterization of the samples also will be determined. © 2000 Kluwer Academic Publishers

1. Introduction

The properties of magnetic materials depend on chemical composition, manufacture, and heat treatment. Some properties, such as saturation-magnetization, change only slowly with chemical composition and they are usually unaffected by manufacturing or heat treatment. However, permeability, coercive force, and hysteresis loss are highly sensitive and show extreme changes among all the physical properties, when changes are made in impurities or heat treatment [1].

FeSi alloys with low Si content have been largely studied due to their soft magnetic properties [1], which make these alloys of great interest from the technological applications point of view, for example in large electrical machines. These alloys present low values for the coercivity giving rise to a reduction in energy losses and high saturation magnetization, close to the value for the pure Fe. Besides this, in grain oriented silicon steels, the improvements of magnetic properties are related to improving the secondary recrystallization texture [2, 3]. In addition, the cost for the Fe based alloys is much lower than other magnetic alloys with similar soft magnetic properties as Co based compounds.

In the current work, the mechanical spectroscopy behaviour in commercial grain oriented silicon steel (GOSS) has been shown. Damping and modulus were measured as a function of temperature from 500 to 1120 K. A study of damping against strain amplitude was also carried out. The general features of the damping spectrum were determined. Furthermore, a possible physical mechanism controlling the jump in the elastic modulus will be proposed.

Magnetic and calorimetric measurements were also carried out to complement the internal friction data.

2. Experimental procedure

Two different kinds of commercial grain oriented silicon steel (GOSS) alloys, called S1 and S2, were checked in the as-received state. As-received state means that the samples were studied in the thermo-mechanical state commercially provided, i.e. they are ready for being employed in transformers. The orientation of these samples was $\{110\}(100)$, cube on face, cube on edge, which was checked by means of etch pitting [4]. The chemical composition determined by

TABLE I Sample composition in wt%, determined by chemical analysis

	Si	C	Ni	Mn	S	V	Co	Cr	Mo	P
S1	2.65	0.017	0.094	0.05	0.001	—	—	—	—	Low
S2	3.09	0.02	—	0.088	0.001	—	—	—	—	Low

TABLE II Characteristic structure of the specimens S1 and S2 in the as-received thermomechanical state

Sample	Structure characteristics	Grain boundary characteristics	Precipitates
S1	Few larger grains, about 10–15 mm Grains of minor size watched with 2000X and 10X Incomplete secondary recrystallization	Narrower than in sample S2, watched with 2000X and 10X	NITAL 5: particles of size 5 μm PIRCAL: particles watched with 1600X. Precipitates of Fe_3C with size between 3 and 5 μm at the grain boundaries. Few inside of the grains Narrow particles at grain boundaries Holes in inner part of the grains with inclusions containing Al and Mg
S2	Larger grains about 10–15 mm, very few small grains	Wider than in sample S1, without precipitates	Any one

TABLE III Mechanical and magnetic characteristic values for S1, S2. The subscripts sp and stp are related to the solvent and solute damping peaks respectively

Sample	$T_{\text{sp}} \text{ (K)}/D(T_{\text{sp}})$	$T_{\text{stp}} \text{ (K)}/D(T_{\text{stp}})$	$T_c \text{ (K)}$	HV
S1	800/0.003	960/0.040	1043	194
S2	780/0.001	900/0.002	1025	197

chemical analysis is shown in Table I. The characteristics of the checked samples are summarised in Table II. In the table the thickness of the grain boundary was compared qualitatively employing the same metallographical study for both samples. These results were labelled as narrower or wider grain boundaries.

Curie temperature, T_c , of samples was determined by means of a magnetometer working at around 70 kA m^{-1} .

The average value of Vickers micro-hardness (HV) results, for each sample of Table I, considering an indenting matrix of 4×10 points, is also written in Table III.

Coercive force, H_c , of the samples was determined from the magnetic induction, J , vs. applied magnetic field, H , hysteresis loops. The measurements were performed at room temperature using a conventional induction system, with triangular wave excitation at five different frequencies (0.125, 1.25, 12.5, 50 and 125 Hz).

The thermal evolution of the magnetization, $M(T)$, has been obtained for the two samples by means of a Manics DSM-8 Faraday magnetometer, at $H = 80 \text{ kA m}^{-1}$. The temperature range used for these measurements is between room temperature and 973 K, which is the highest temperature limit for the used device.

Mechanical spectroscopy measurements were carried out employing an inverted torsion pendulum which works at frequencies between 0.2 and 40 Hz, under high vacuum of the order of 10^{-7} Torr in the sample environment. The device is controlled by an automatic data acquisition system based on a PCL 812 card [5, 6]. The maximum strain on the sample, ε_m , was less than 5×10^{-5} . The heating and cooling rates were of 1 de-

gree per minute. The damping, D , was measured with an error less than 2% [7]. The measured damping values were amplitude dependent, but these values were not corrected to the intrinsic damping [8], since the measured shape of the damping spectra changes very slowly and therefore it does not obstruct the subsequent analysis.

However, amplitude dependent damping (ADD) effects were carefully checked as a function of temperature. The freely decaying torsional amplitudes A_n , $n = 0, 1, 2, \dots, N$ were measured at constant temperature by means of a data acquisition system. The temperature during this decaying was kept constant with a stability of $\pm 0.2^\circ\text{C}$. On a first step, polynomials were fitted to the data $\ln(A_n)$ vs. n representing the decaying oscillations. The damping as a function of amplitude was determined by the first derivative of the polynomial $\ln(A_n)$ against n . The results were depicted as damping, D , against maximum strain on the sample, ε_m . Best fits were obtained with polynomials of degree ≤ 3 . The amplitude dependent damping degree was determined through the slope of $D(\varepsilon_m)$ curves, $s = dD/d\varepsilon_m$. This may be replaced in a restricted range of ε_m by the mean value $S = \Delta D/\Delta\varepsilon_m$ [9]. It should be pointed out, that the linearity of the oscillating amplified signal response during the decaying oscillations was accurately checked. This linearity can be assured up to $A_0/A_n = 10,000$ ratios. In fact, this point is crucial for an accurate checking of ADD effects.

Differential thermal analysis (DTA) studies were performed in a SETARAM apparatus model TGDTA 92, under argon purge with a heating rate of 20 degree per minute.

3. Results and discussion

3.1. Magnetic measurements

Figs 1a and b show the hysteresis loops, $(-1 \text{ kA m}^{-1} \leq H_{\text{app}} \leq 1 \text{ kA m}^{-1})$ measured at 0.125, 12.5 and 125 Hz for the samples S1 and S2, respectively. In all the cases the samples seem to be saturated at 9 kA m^{-1} with $J_s \cong 2 \text{ T}$, at room temperature.

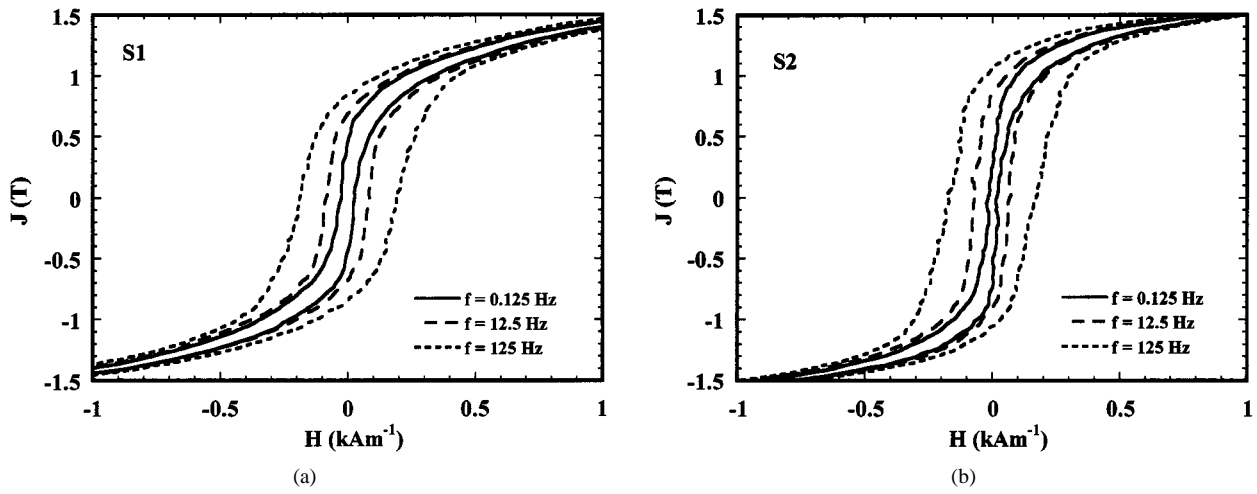


Figure 1 Hysteresis loops corresponding to the samples S1 (a); and S2 (b), measured at 0.125, 12.5 and 125 Hz.

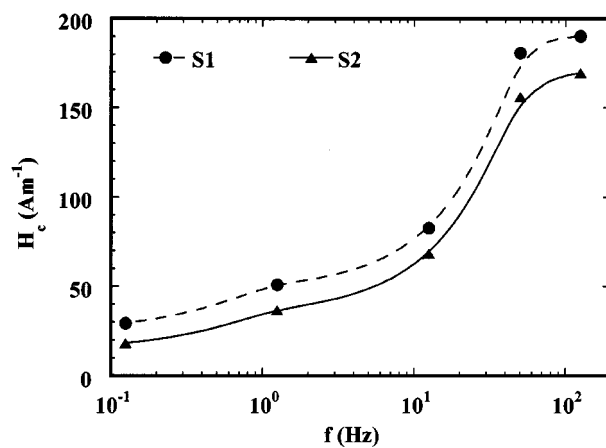


Figure 2 Evolution of the coercive force, H_c , with the excitation frequency for the two samples studied.

An increase in the coercive force with frequency is observed, meanwhile the saturation magnetization does not vary. As a result of sample thickness, the magnetic response of the material to the magnetic applied field is not the same for all the frequencies, due to the difficulty in the penetration of the magnetic field in the sample when increasing the frequency.

The evolution of H_c with frequency, f , for the two studied samples is shown in Fig. 2. Here, it is clearly reflected that the most interesting sample is the S2 with $H_c < 20 \text{ A m}^{-1}$ from the point of view of the magnetic softness, and for applications using low frequencies, meanwhile the value for the H_c in the S1 sample is around 40 A m^{-1} . At higher frequencies of the applied field, all the samples present an increase in the value of H_c reaching values above 150 A m^{-1} for $f = 50 \text{ Hz}$, but for higher frequencies H_c tends to a saturation value about 200 A m^{-1} . For all the frequency ranges studied, S1 sample has values above the ones for the S2 sample which is clearly the softest one.

In Fig. 3, magnetization vs. temperature, T , curves for the two samples together with the corresponding to the pure Fe are represented. Due to the upper temperature limit (973 K) of the magnetometer, Curie temperature, T_c , of the samples could not be determined

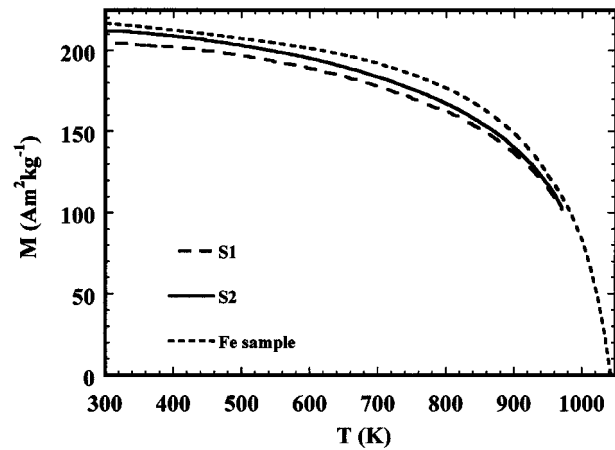


Figure 3 Thermomagnetization curves, $M(T)$, of the two samples compared with the pure Fe curve, measured between room temperature and 973 K.

from these tests. Hence the $M(T)$ curves seem to be very similar to the pure Fe one and due to the high Fe content in the samples (above 97.5 at%) the values for the T_c of the samples will not differ more than 20 K from the ones corresponding to pure Fe (1043 K), as is typical in these Fe-rich FeSi alloys [1]. The differences in the value of the saturation magnetization between the two samples are very small and close to the pure Fe ones. These M values at room temperature (around $200\text{--}210 \text{ A m}^2 \text{ kg}^{-1}$) are always lower than the value for Fe ($\cong 218 \text{ A m}^2 \text{ kg}^{-1}$), as it could be expected. Moreover, due to the small amount of sample used for the measurements ($\cong 2 \text{ mg}$), 1% of error in the weight together with the own error of the experimental device, e.g. the two samples have not been situated exactly at the same position for the measurements, make these differences in the value of M negligible. However, the relative changes in magnetization for the different temperatures in each sample are not subjected to these errors.

It is also noticeable that the $M(T)$ curves are very smooth in the temperature range of the measurements, suggesting the non-occurrence of any changes in magnetic character of the samples or the appearance of new magnetic phases during the heating.

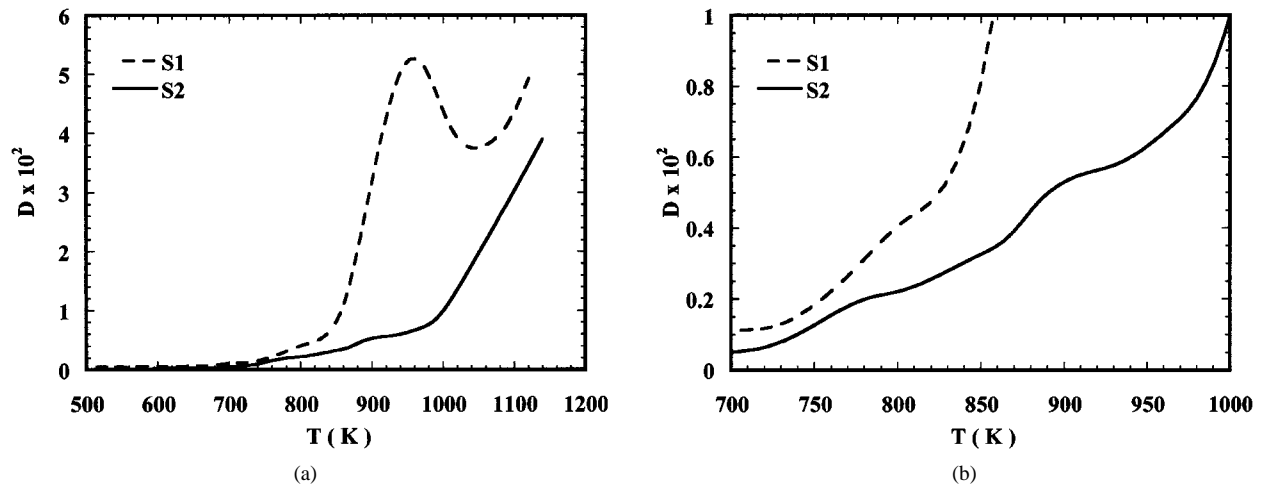


Figure 4 (a) Damping spectra for samples S1 (dashed line) and S2 (full line), during the heating; (b) Zoom of the damping spectra between the temperature range 700–1000 K, for the samples S1 (dashed line) and S2 (full line).

3.2. Mechanical spectroscopy measurements

Fig. 4a shows the mean damping behaviour as a function of temperature for samples S1 and S2 during the heating, plotted by means of dashed and full lines respectively. Fig. 4b shows a zoom of the temperature range between 700 and 1000 K. The damping spectra for both kinds of samples show the solvent damping peak (SP) of the grain boundary relaxation at approximately 780 and 800 K for the S2 and S1 samples, respectively. The height of the SP is lower in the S2 sample than in S1 one, owing to the difference in grain size between the samples. The peak temperatures of SP for both samples agree with the values reported in literature [10, 11]. The peak temperatures, T_{sp} , and heights of SP peaks for both samples were written in Table III.

The solute damping peak (STP) of the grain boundary relaxation at higher temperatures than those of the SP peak also appears for both kinds of samples. The STP peak height is also lower in S2 than in S1, indicating that S1 has a larger grain size and a more inhomogeneous distribution of grain size than S2 (see Table II).

The peak temperature determination of a relaxation peak overlapped on other peaks and also on the background, can only be made in an approximate mode. Moreover, the decomposition of the spectra is not unique [12]. However, we propose, that these damping values at SP and STP peak temperatures can be employed as a testing parameter of the grain size and its morphology.

The moduli behaviours for the samples S1 and S2 are plotted in Fig. 5. The dotted line represents the modulus behaviour during the cooling for a sample S1.

The modulus behaviour for S1 shows a practically constant value up to 760 K followed by a jump towards higher values during heating. Furthermore, from 870 K the modulus decreases on increasing temperature. In contrast, for sample S2 the modulus remains practically constant until 850 K and decreases on increasing temperature, but the jump-up in the modulus does not appear.

By watching carefully the jump in the modulus which appears for S1, two hills can be observed on it. As

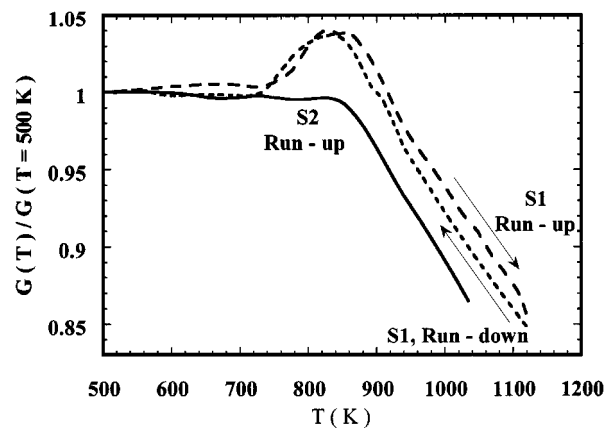


Figure 5 Moduli behaviour for the samples S1 (dashed line) and S2 (full line) during heating. Dotted lines represent the elastic modulus for sample S1 during cooling after having reached the highest temperature during the test.

it was already mentioned, the difference between the microstructures of S1 and S2 leads to different damping spectra. In fact, the different moduli behaviours are also produced by the differences in the microstructure. S1 has an incomplete secondary recrystallization (Table II), meanwhile this problem does not appear for S2.

The temperature of the jump in the modulus is closer to the recrystallization temperature reported for GOSS, Fe-Si based alloys and also for iron [2, 3, 13, 14].

It should be mentioned that the study of any physical phenomena by means of anelastic techniques in this range of temperatures is very complicated due to the overlapping of the following damping peaks: recrystallization; precipitation; grain boundaries and non-homogeneous microstructure; i.e. an arrangement of small grains bounded by larger grains [13–15]. However, an enough clear splitting of each effect could be made in the present work.

The beginning of the modulus jump and the first hill can be mainly related to the recrystallization process of the incomplete secondary recrystallization. The second hill, at higher temperatures, can be related to the appearance of a precipitation process. In fact, the effects of the fine precipitation or cluster formation is very important

on the recrystallization rate [3]. Moreover, in deformed Fe-Si alloys containing nitrogen, Si_3N_4 precipitates appear at the boundaries of the growing grains [13]. The discussion on the precipitation process will be made in a further work. The recrystallization mechanism associated to the jump in the S1 modulus is in agreement with the behaviour of the S2 modulus. In fact, S2 samples do not have an incomplete secondary recrystallization and therefore, a jump in the modulus does not appear.

On the other hand, it must be pointed out that the modulus shows a jump-down during the cooling after the sample has reached 1120 K. This kind of behaviour is opposite to the expected, and also reported on [13], for the modulus evolution during recrystallization. During the heating, the jump-up appears by the appearance of stresses by the growth of newly oriented strainfree grains, but during the cooling a jump-down in the modulus is not expected since after the recrystallization temperature, the recrystallized structure is already formed by new strain-free grains.

The physical driving force which controls this reversible jump could be related to an interaction process between the dislocations and obstacles as solutes or small precipitates. Besides this, the dislocations at the grain boundaries could be cooperating in the proposed physical mechanism, as it will be discussed in the following paragraphs.

When the boundary moves, the solute atoms migrate along with the boundary and exert a drag that reduces the boundary velocity. The magnitude of the drag will depend on the binding energy and on the concentration in the boundary [16]. During recrystallization, the dislocations are absorbed by the boundary which separates it from the new grain, they are decomposed into infinitesimal dislocations, diffuse rapidly and annihilate with similarly absorbed dislocations of the opposite sign [17].

At temperatures lower than that of the recrystallization, the mobilities of the grain boundaries and the dislocations are small. On the contrary, at the beginning of the recrystallization, the grain boundary migration is important. Moreover, the increase in temperature leads also to an increase in the dislocations mobility.

The dragging of defects by dislocation can produce an inverse modulus defect as it was demonstrated by Simpson and Sosin [18]. Moreover, the appearance of dragging processes at relatively higher temperatures was recently reported by Lambri *et al.* [19].

The study of the S parameter as a function of temperature gives an important information on the behaviour of the dislocations in the structure, even if the ADD degree is small [20]. Fig. 6 shows the behaviour of the S parameter against temperature for both kinds of samples. The ADD effects do not appear until temperatures closer to the recrystallization one, around 800 K, for sample S1. In contrast, for S2 the temperature where the ADD effects appear, coincides with the temperature at the beginning of the modulus decrease, about 850 K. In other words, the S values are different from zero at lower temperatures for S1 than for S2, in agreement with the hypothesis above proposed. In fact, in the S1 samples the beginning of the recrystallization

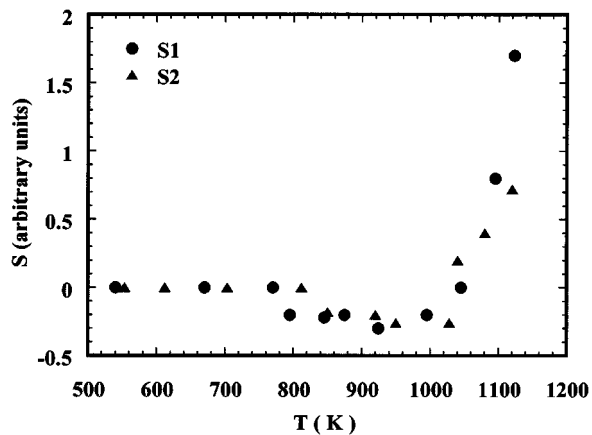


Figure 6 $S = \Delta D / \Delta \varepsilon_m$ parameter against temperature for samples S1 and S2.

enhances the dislocation mobility, earlier than for S2 samples that have a complete secondary recrystallization. The beginning of the ADD effects is related to the capacity of dislocations to overcome the weak obstacles. In ADD measurements the dislocations are only forced to overcome the weak obstacles, and not the strong ones [21–23]. In this process the increase of energy of the dislocation line by thermal agitation is very important, as it was pointed out by Friedel [17].

The S values equal to zero until temperatures closer to the recrystallization one and also to the beginning of the decrease of the modulus on increasing temperature, could be related to the existence of internal stresses which give rise to a dislocation pinning. At higher temperatures the lattice recovery and the increase in the thermal energy of dislocations lines allow the dislocations to overcome the barriers and then they can move. In fact, internal stresses produced by the manufacturing process can remain despite the recrystallization, as it was pointed out by Anderson *et al.* for Fe-Mn-Si alloys [24].

The S parameter is negative within the temperature ranges between the recrystallization and the Curie transition. At temperatures higher than the Curie point, S increases towards positive values. This negative dependence of the ADD is related to magnetostrictive effects. Meanwhile, the positive dependence in the paramagnetic zone could be related to the micro yield behaviour of dislocation lines.

The internal friction is expressed as $\Delta E / 2\pi E$, where E is the vibration energy and ΔE is the energy consumed per cycle. When the vibrational stress is acting, the vibration energy is proportional to the square of the amplitude, and the consumed energy corresponds to the hysteresis loss caused by irreversibility [25]. The characterization of mechanical spectroscopy spectrum in ferromagnetic alloys is complicated, since both the dislocation and grain boundary structures, and magnetic processes contribute to the total damping and modulus values [26]. The damping in ferromagnetic alloy is caused by the irreversibility of magnetization. A rearrangement, such as the movement of the domain walls, occurs due to the reverse effect of magnetostriction [25]. Therefore, this increase in the vibrational

energy produced by the coercive force leads to the decrease in the damping on increasing strain showed in Fig. 6 within the ferromagnetic range.

In contrast, the magnetization vectors of the individual domains in the paramagnetic range are randomly oriented and consequently, the cyclic stress introduces only a cyclic elastic strain without a cyclic magnetostrictive strain component, giving rise to a positive dependence of ADD owing to the thermal assisted break away of dislocations.

Considering again the behaviour of the elastic modulus (Fig. 5) for temperatures higher than 850 K for both kinds of samples, the moduli decrease on increasing the temperature. These temperatures, where a normal dependence of the elastic modulus as a function of the temperature is reestablished, agree with the results reported by Matsuo [3], for the recovery temperature of the lattice strain. Therefore, when a larger quantity of stresses on the lattice has relaxed a normal dependence of the modulus is reestablished.

3.3. DTA measurements

The effect of the incomplete secondary recrystallization can be analysed from the DTA measurement performed, during the first heating, for the S1 sample; Fig. 7. As it can be seen in the figure, the change in the base line related to the Curie point appears. The Curie point is in agreement with the one obtained by means of magnetic measurements and the reported values [1]. Besides this, it seems that another peak appears at around 850 K, but it is difficult to determine. The evolution of this peak in the different run-ups in temperature is even more complicated and unclear. The lack of resolution in the thermograms for determining the incomplete secondary recrystallization evolution, could be related to the small signal expected from this phenomenon if compared with the signal emitted by the whole matrix [27].

In short, the mechanical spectroscopy, considering also amplitude dependent damping must be taken as a very suitable technique for studying the evolution of these small processes related to the incomplete secondary recrystallization in GOSS, which cannot be appreciated by calorimetric or magnetic measurements.

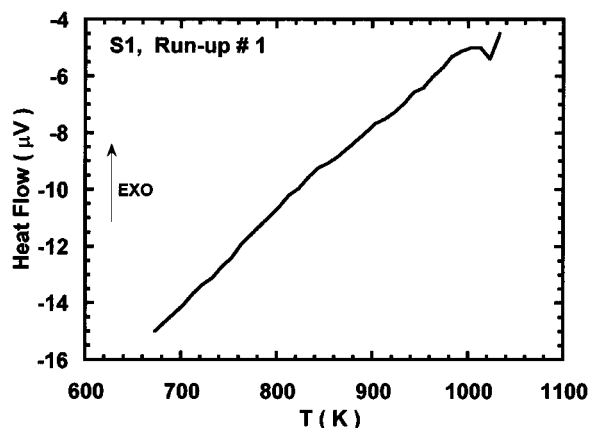


Figure 7 DTA thermogram of a sample S1 for the first run-up in temperature.

4. Conclusions

Mechanical spectroscopy and amplitude dependent damping measurements resulted to be quite suitable for studying the recrystallization evolution in GOSS. Moreover, this technique was more appropriate than the differential thermal analysis.

A contribution of the dislocations for controlling the anomalous jump in the elastic modulus which appears in samples with incomplete secondary recrystallization was proposed.

The outstanding features of the damping and the modulus spectra might be employed as the characterization parameters of the microstructural state and its evolution during thermomechanical treatments.

Acknowledgements

This work was partially supported by the PEI 0116/98 of the National Council of Research (CONICET), the Escuela de Ingeniería Eléctrica of the Faculty of Science and Engineering of the Rosario National University and the PID 202/98 de la UNR. We wish to express our thanks to E. Brandeleze and G. Mansilla for the data about the samples characterization written in Table II.

References

1. R. M. BOZORTH, "Ferromagnetism" (D. Van Nostrand Company, Inc., 1964).
2. Y. INOKUTI, F. SAITO and C. GOTTOH, *Mater. Trans. JIM* **37**(3) (1996) 203.
3. M. MATSUO, *Trans. Iron Steel Inst. Japan* **29** (1989) 809.
4. R. TINIVELLA, G. MANSILLA, E. BRANDELEZE and O. LAMBRI, in Proceeding of the First Argentine Meeting on Magnetic Materials and their Applications (Argentine Society of Metals, Cordoba, Argentina, 1995) p. 61.
5. O. A. LAMBRI, PhD thesis, Rosario National University, 1993.
6. O. A. LAMBRI, *Mater. Trans. JIM* **35**(7) (1994) 458.
7. *Idem.*, *J. Phys IV* **6** (1996) 313.
8. B. J. LAZAN, "Damping of Materials and Members in Structural Mechanics" (Pergamon Press, 1968).
9. B. J. MOLINAS, O. A. LAMBRI and M. WELLER, *J. of Alloys and Comp.* **211/212** (1994) 181.
10. Y. IWASAKI and K. FUJIMOTO, *J. Phys. (Paris)* **42** (1981) C5-475.
11. F. POVOLO and B. J. MOLINAS, *Il Nuovo Cim* **14D**(2) (1992) 287.
12. I. G. RITCHIE, private communication.
13. B. BEYER, E. M. HERBST and J. WIETING, *Mat. Sci. Forum* **119-121** (1993) 385.
14. M. L. BERSTEIN and E. S. TIKHOMIROVA, in "Relaxation Phenomena in Metals and Alloys," edited by B. Finkelstein (Consultants Bureau, New York, 1963) p. 211.
15. R. MULYUKOV, S. MIKHAILOV, R. ZARIPOVA and D. SALIMONENKO, *Mat. Res. Bull.* **31** (1996) 639.
16. D. A. PORTER and K. E. EASTERLING, "Phase Transformations in Metals and Alloys" (Van Nostrand Reinhold International, 1988).
17. J. FRIEDEL, "Dislocations" (Pergamon Press, 1964).
18. H. M. SIMPSON and A. SOSIN, *Phys. Rev. B* **16**(4) (1977) 1489.
19. O. A. LAMBRI, G. I. LAMBRI, M. E. TORIO and C. A. CELAURO., *J. Phys. Condens. Matter* **8** (1996) 10253.
20. O. A. LAMBRI, A. PEÑALOZA, A. V. MORÓN-ALCAIN, M. ORTIZ and F. C. LUCCA, *Mat. Sci. and Eng. A* **212** (1996) 108.
21. A. GRANATO and K. LÜCKE, *J. Appl. Phys.* **27** (1956) 583.
22. R. B. SCHARWZ and L. L. FUNK, *Acta Metall.* **31**(2) (1983) 299.

23. R. B. SCHWARZ, *J. Phys.* **46** (1985) C10–207.
24. M. ANDERSON, J. VAN HUMBEECK and J. ÁGREN, *Mater. Trans. JIM* **37**(7) (1996) 1363.
25. M. HINAI, S. SAWAYA and H. MASUMOTO, *ibid.* **35**(1) (1994) 74.
26. F. P. HIGGINS and S. H. CARPENTER, *Mater. Sci. and Eng.* **37** (1979) 173.
27. J. SESTÁK, in “Comprehensive Analytical Chemistry” edited by G. Svehla (Elsevier, 1984).

*Received 3 September 1998
and accepted 21 June 1999*